Continental Shelf Research, Vol. 13, No. 11, pp. 1183–1204, 1993.
Printed in Great Britain.

0278-4343/93 $6.00 + 0.00

The generation of offshore tidal sand banks and sand waves

SUZANNE J. M. H. HULSCHER,*† HUIB E. DE SWART*
and HUIB J. DE VRIEND†

(*Received* 3 *May* 1993; *accepted* 5 *July* 1993)

Abstract—A simple morphological model is considered which describes the interaction between a tidal flow and an erodible bed in a shallow sea. The basic state of this model describes a spatially uniform tide over a flat bottom where the flow vector is represented as a tidal ellipse. The linear stability of this solution is analysed with respect to bed form perturbations. Results are presented for both a uni-directional and circular tide. In the former case the wave-length and the orientation of the fastest growing bed mode agree well with those of tidal sand banks. However, this model only predicts the growth of large-scale sand ridges. With a simplified numerical model we tentatively show that the effects of secondary currents on the sediment transport trigger the formation of instabilities at an essentially smaller scale, *viz*, sand waves. Another limitation of a model with uni-directional tides is that no selective modes found are the first to become unstable if the model parameters are varied. In the case of a circular tide, critical model parameters are found below which the basic state is stable. We conclude that this provides a starting point for the development of a weakly non-linear analysis, which will yield information on the amplitude behaviour of marginally growing bed forms.

1. INTRODUCTION

IN many shelf seas with strong tidal currents, undulations of the sea bed are observed which have horizontal length scales much larger than the local water depth. Often a distinction is made between sand waves and sand ridges. The former features have typical wave-lengths of ten times the local water depth, their crests are perpendicular to the direction of the principal tidal currents and they migrate several metres per year (STRIDE, 1982; LANCKNEUS and DE MOOR, 1991). On the other hand sand banks have characteristic wave-lengths of 100 times the undisturbed water depth, they hardly move and their crests are orientated slightly anticlockwise (angles between 5 and 30°) with respect to the principal tidal current direction (Fig. 1; see also VAN ALPHEN and DAMOISEAUX, 1989; PATTIARATCHI and COLLINS, 1987).

In general the height of sand waves and ridges is between 4 and 10 m, but there are examples in which the height of the ridges can reach values up to 30 m, see OFF (1963).

Understanding the dynamics of these large-scale bed forms is of interest from a practical as well as a scientific point of view. It was already noted by OFF (1963) that the presence of sand waves and sand ridges is highly correlated with the occurrence of intense tidal

*Institute for Marine and Atmospheric Research, Utrecht University, Princetonplein 5, 3584 CC Utrecht, The Netherlands.

†Delft Hydraulics, p.o. box 152, 8300 AD Emmeloord, The Netherlands.

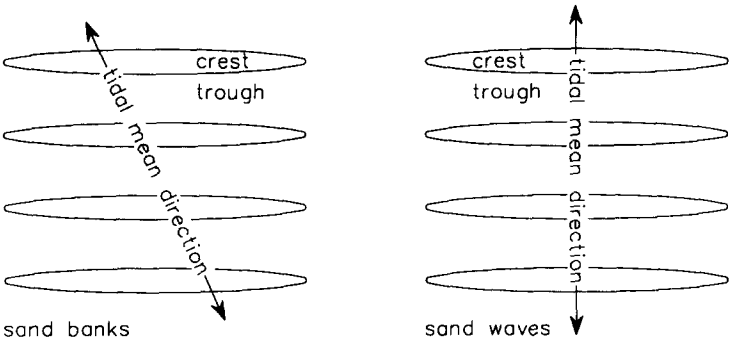

Fig. 1. A sketch of the position of sand waves and tidal ridges with respect to the principal tidal axis.

currents. Moreover, the observation that their horizontal length scales are clearly distinct from the tidal wave-lengths suggests that the formation of sand waves and sand ridges (also referred to as linear sand banks or tidal ridges) may be explained as free instabilities of a dynamic morphological system in which tidal currents and the sea-bottom interact, leading to evolution of these bed forms. This hypothesis was first investigated in detail by HUTHNANCE (1982a,b). His model consists of the depth-integrated shallow water equations, a continuity equation for the sediment and a simple parameterization for the sediment transport. He studied the behaviour of small bottom perturbation evolving on a basic state consisting of a uni-directional tide and a flat bottom. The model predicts that there is a preferred initial growth of bed form perturbations with their crests turned slightly anticlockwise with respect to the current direction. A physical explanation of this effect was already give by ZIMMERMAN (1981) and ROBINSON (1981). The predicted wave-lengths and orientations were in fairly good agreement with observations. A variant of this model was discussed by DE VRIEND (1990), who replaced the local bed load parameterization with a suspended load transport including settling lag effects, and incorporated the effects of wave stirring and wave-asymmetry.

In this paper a modified version of the HUTHNANCE (1982a,b) model is derived and analysed. The introduction of this new model is motivated by two observations. First, the original model does not describe the presence of a critical mode with a finite wave-length, which is the first mode to become unstable if a parameter (like tidal current amplitude, friction parameter) is varied. This appears to be contrary to observations which show that if tidal amplitudes are too small or the water depths become too large no bed forms are to be expected. Secondly, the model of HUTHNANCE (1982a,b) only predicts the formation of sand ridges, but no sand waves are found. This is probably because the vertical structure of the currents is neglected, by implication of the depth integration. However, the flow accelerations, induced by the ridges, will generate secondary circulations in the vertical plane which affect the direction of the sediment transport. In this study the HUTHNANCE (1982a,b) model will be modified by allowing for elliptical tidal currents and by adjusting the sediment flux to allow for the effect of secondary currents. It will be demonstrated that elliptical tides imply the presence of critical parameter values at which a specific perturbation first starts to grow exponentially. The modified sediment transport parameterization will be shown to predict the formation of both sand waves and sand ridges.

The practical relevance of this model lies in the offshore industry and in the maintenance of navigation channels. A pipeline on a bed with sand waves may have large spans, and under certain conditions it may even buckle up or break. Therefore, pipelines in such areas are usually buried at a certain depth below the minimum expected trough level of the sand waves, which is an expensive operation. A better knowledge of sand wave behaviour may lead to substantial savings here. For the maintenance of shipping channels it is important to know how fast sand banks and sand waves are moving and what amounts of sediment they may deposit in the channel. Besides, they may influence the minimum navigation depth.

The organization of this paper is as follows. In section 2 we present the model equations which are the shallow water equations, supplemented with a bottom evolution equation and a parameterization of the sediment transport. The motivation to use such a simple model is that we are mainly interested in the basic interaction mechanisms between tidal currents and bed form changes. Subsequently characteristic scales of motion are introduced and the equations of motion are formulated in a non-dimensional form. Based on the observation that the morphological time scale is much larger than the tidal period the equations are further simplified. In the resulting model the bottom evolution is determined by the tidally averaged fluxes of sediment and the bottom variable may be considered as time independent in the flow equations. In section 3 the linear stability concept is described and a basic state is derived. The latter describes a spatially uniform tidal flow over a flat bottom. The stability of this basic state with respect to arbitrary bed flow perturbations is investigated in section 4. It is demonstrated that the flow responds in all overtones of the basic tidal frequencies, including the residual component. The exact solutions of the flow response are difficult to analyse, but it is shown that they can be fairly well approximated by solutions obtained with a harmonic truncation method.

In section 5 the morphodynamic response with respect to the disturbed flow field is investigated by computing the initial growth rates of the bed form perturbations. Results are shown both for a uni-directional and circular tide. It is then observed that this model is able to explain the formation of tidal sand ridges, but no sand waves are found. Therefore, in section 6 the effect of secondary currents is taken into account and it is demonstrated that they cause the generation of both ridges and sand waves. We end with some conclusions in the final section.

2. MODEL

Unsteady flow, sediment transport and bed evolution in shallow seas can be described with the following model

$$\frac{\partial u}{\partial t} + u\frac{\partial u}{\partial x} + v\frac{\partial u}{\partial y} - fv = -g\frac{\partial \zeta}{\partial x} - r\frac{u}{H - h + \zeta}, \tag{1}$$

$$\frac{\partial v}{\partial t} + u\frac{\partial v}{\partial x} + v\frac{\partial v}{\partial y} + fu = -g\frac{\partial \zeta}{\partial y} - r\frac{v}{H - h + \zeta}, \tag{2}$$

$$\frac{\partial(\zeta - h)}{\partial t} + \frac{\partial}{\partial x}[(H + \zeta - h)u] + \frac{\partial}{\partial y}[(H + \zeta - h)v] = 0, \tag{3}$$

$$\frac{\partial h}{\partial t} + \vec{\nabla} \cdot \vec{S_b} = 0, \tag{4}$$

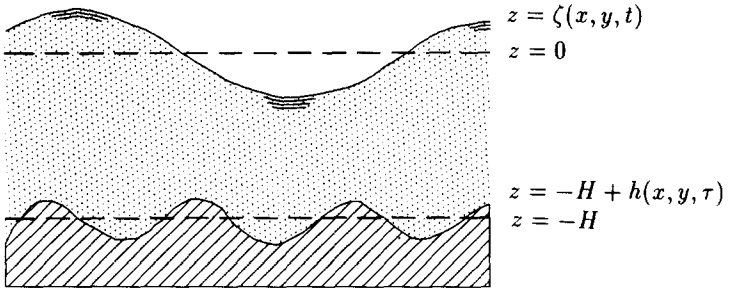

Fig. 2. Sketch of the model geometry (side view).

$$\vec{S_b} = \alpha |\vec{u}|^b \left\{ \frac{\vec{u}}{|\vec{u}|} - \lambda \vec{\nabla} h \right\}. \tag{5}$$

Here u and v are the velocity components in the x- and y-direction, $z = \zeta$ is the free surface elevation and h is the bottom level with respect to the undisturbed water depth H (see Fig. 2).

The x-axis is chosen in the direction of the principal current. Furthermore
f: Coriolis parameter;
r: linearized friction parameter;
α: constant (includes effect of porosity);
b: power of transport (usually 3–5);
λ: constant (usually 1–3).

The model consists of three parts: a description of the fluid motion, a description of the sediment motion and a sediment balance. In order to make this model as simple as possible we take the boundaries infinitely far away. This means that the model considers situations far offshore.

The fluid motion is described by the depth averaged shallow water equations (1)–(3). We assume no wind stress at the sea surface and a shear stress at the bottom which depends linearly on the mean flow velocity. The behaviour of the bottom is based on mass conservation of the sediment equation (4). As velocities are not very large we assume that the sediment transport may be considered as bedload. We can parametrize bedload transport by an empirical relationship. The one we have chosen, equation (5) is a generalization of a class of widely used transport formulae, see VAN RIJN (1989). This expression describes that transport increases with increasing velocities and that the sediment is transported easier downhill than uphill. Equation (5) does not include a threshold. Including a threshold in the parametrization of the sand transport can be done but it turns out not to affect the model results qualitatively. This model only is a study of a mechanism so including a threshold does not give more information. In order to keep the model as simple as possible we decided not to include a threshold in the sediment transport formula.

In general, equations (1)–(5) are too difficult to analyse. Therefore it becomes worthwhile to investigate whether specific terms can be neglected in the first instance. A convenient method is to rewrite the equations in a non-dimensional form and subsequently search for small parameters. First we note that there are two length scales involved in this problem. One is the tidal wave-length L, the other is the tidal excursion length $l_m = U/\sigma$ in which σ is the tidal frequency and U the tidal current amplitude. Since we are interested in

the behaviour of ridges which, according to observations, have length scales of the order of the tidal excursion, we scale the spatial coordinates with the tidal excursion. Since currents typically vary over a tidal period we scale t with σ^{-1}. Furthermore we note that there is a second time scale involved in this problem which is the morphological time scale T_m, at which we expect the sand banks to grow. The scale for the free surface elevations ζ follows from the typical momentum balance for a tidal wave. The previous considerations motivate the introduction of the following nondimensional variables (denoted by $_*$):

$$\vec{u} = U\vec{u}_* \tag{6}$$

$$t = \frac{t_*}{\sigma} \tag{7}$$

$$\vec{x} = l_m \vec{x}_* \tag{8}$$

$$h = Hh_* \tag{9}$$

$$\zeta = \frac{UL\sigma}{g}\zeta_* \tag{10}$$

When introducing this scaling into the original equations, using the dispersion relation

$$L\sigma = \sqrt{gH}. \tag{11}$$

for a shallow water wave and finally dropping the asterisk ($_*$), we arrive at

$$\frac{\partial \zeta}{\partial x} + \delta\left\{\frac{\partial u}{\partial t} + u\frac{\partial u}{\partial x} + v\frac{\partial u}{\partial y} - \hat{f}v\right\} + \frac{\delta \hat{r}u}{1 + \delta\zeta - h} = 0 \tag{12}$$

$$\frac{\partial \zeta}{\partial y} + \delta\left\{\frac{\partial v}{\partial t} + u\frac{\partial v}{\partial x} + v\frac{\partial v}{\partial y} - \hat{f}u\right\} + \frac{\delta \hat{r}v}{1 + \delta\zeta - h} = 0 \tag{13}$$

$$\delta\frac{\partial \zeta}{\partial t} - \frac{\partial h}{\partial t} + \frac{\partial}{\partial x}[(1 - h + \delta\zeta)u] + \frac{\partial}{\partial y}[(1 - h + \delta\zeta)v] = 0 \tag{14}$$

$$\frac{\partial h}{\partial t} = -\hat{\alpha}\vec{\nabla}\cdot\left\{|\vec{u}|^b\left[\frac{\vec{u}}{|\vec{u}|} - \hat{\lambda}\vec{\nabla}h\right]\right\}, \tag{15}$$

in which we have defined the dimensionless parameters:

$$\delta = \frac{U}{\sigma L} = \frac{l_m}{L} \tag{16}$$

$$\hat{r} = \frac{r}{\sigma H} \tag{17}$$

$$\hat{f} = \frac{f}{\sigma} \tag{18}$$

$$\hat{\lambda} = \lambda\frac{H\sigma}{U} \tag{19}$$

$$\hat{\alpha} = \frac{\alpha U^b \sigma}{Hl_m} = \frac{1}{\sigma T_m}, \tag{20}$$

where T_m follows from a balance of the two terms in the bottom evolution (4) and may be interpreted as the morphological time scale.

The maximum tidal velocity is of the order of 1 m s^{-1}. The frequency of the M_2-tide in the North Sea $\sigma = 1.4\,10^{-4}\,s^{-1}$. These two make the morphological length scale about 7 km. The linearized friction coefficient r can be estimated from the drag coefficient C_d following ZIMMERMAN (1982). The value for the drag coefficient C_d in a shallow sea is between 0.01 and 0.001. Assuming a depth of 30 m we find that $\hat{r}$ varies between 0.237 and 2.37. Taking a Coriolis parameter at 52°N we have $f \simeq 1.16\,10^{-4}\,s^{-1}$, which implies $\hat{f} \simeq 0.8$. In the North Sea the tidal wave-length is in the order of hundreds of kilometres, which means the parameter δ is small, $\delta \simeq 0.01$. The exponent in the bedload transport formula, b, is usually taken between 3 and 5. It can be shown that λ can be interpreted as the inverse of the tangent of the angle of no respose of the sand. As such angle ranges theoretically from 30° to 90°, λ ranges from 0 to $\sqrt{3}$. Usually the parameter $\hat{\alpha}$, which may be computed from VAN RIJN (1989), is very small ($\mathcal{O}(10^{-6})$), which yields the morphological time scale

$$T_m \simeq 200 \text{ yr}. \tag{21}$$

It is then obvious that the bottom variable h will hardly vary on the tidal time scale, so we may put $\partial h/\partial t = 0$ in the momentum and continuity equations. Furthermore, the slow evolution of the bed is not directly determined by the details of the sediment transport within a tidal cycle, but rather by the net, i.e. tidally averaged, sediment fluxes. The mathematical foundations of this approach follow from the theory of averaging which is discussed in SANDERS and VERHULST (1985), also see KROL (1991). Application of this theory to the present model implies that the bottom variable is considered to be only a function of the slow morphological time variable $\tau = \hat{\alpha}t$, whereas the bottom equation (15) is replaced by

$$\frac{\partial h}{\partial \tau} = -\vec{\nabla} \cdot \left\langle \left\{ |\vec{u}|^b \left[\frac{\vec{u}}{|\vec{u}|} - \hat{\lambda} \vec{\nabla} h \right] \right\} \right\rangle \tag{22}$$

with the brackets denoting a tidal average. The averaging theorem guarantees that equation (22) is an $\mathcal{O}(\alpha)$ approximation of the original bottom equation (15) at the morphological time scale. In order to compute the net sediment fluxes S_x and S_y we have to solve the flow equations at the fast time scale, where $\partial h/\partial t = 0$. So the equations of motion to be considered from now on are (12), (13) and (14) with $\partial h/\partial t = 0$, supplemented with (22).

3. LINEAR STABILITY CONCEPT AND BASIC STATE

3.1. *Linear stability theory*

As already noted in the introduction of this paper we investigate whether the presence of tidal sand banks and sand waves may be explained as free instabilities of a morphological system. This hypothesis can be tested by first defining a basic state which describes a tidal current over a flat bottom. The next step is to introduce bed perturbations with arbitrary wavenumbers in the horizontal directions. Subsequently we study the initial interaction between bed forms and currents and determine whether the perturbations are amplified or reduced. A basic state, considered for fixed model parameters, is said to be stable if arbitrary bed form disturbances with non-zero wavenumbers decay exponentially. This

implies that all perturbations have negative growth rates. Conversely, if there is at least one perturbation with a positive growth rate the basic state is unstable.

From a mathematical point of view this may be formulated as follows. The solution of the problem is symbolically written as the vector

$$\psi = (u,v,\zeta,h). \tag{23}$$

Now we consider the response of the system if a small wave-like perturbation in the bottom is prescribed as an initial state. In this way we investigate the stability of the basic state. If the amplitude of the perturbation with respect to the undisturbed water depth is denoted by γ, then an approximate solution can be written as:

$$\psi = \psi_0 + \gamma\psi_1 + \gamma^2\psi_2 + \ldots . \tag{24}$$

Here ψ_0 corresponds with the basic state which describes a flow over a flat bottom, i.e.

$$\psi_0 = (u_0, v_0, \zeta_0, 0). \tag{25}$$

u_0, v_0 and ζ_0 must obey

$$\frac{\partial\zeta_0}{\partial x} + \delta\left\{\frac{\partial u_0}{\partial t} + u_0\frac{\partial u_0}{\partial x} + v_0\frac{\partial u_0}{\partial y} - \hat{f}v_0\right\} + \frac{\delta\hat{r}u_0}{1+\delta\zeta_0} = 0 \tag{26}$$

$$\frac{\partial\zeta_0}{\partial y} + \delta\left\{\frac{\partial v_0}{\partial t} + u_0\frac{\partial v_0}{\partial x} + v_0\frac{\partial v_0}{\partial y} + \hat{f}u_0\right\} + \frac{\delta\hat{r}v_0}{1+\delta\zeta_0} = 0 \tag{27}$$

$$\delta\frac{\partial\zeta_0}{\partial t} + \frac{\partial}{\partial x}[(1+\delta\zeta_0)u_o] + \frac{\partial}{\partial y}[(1+\delta\zeta_0)v_0] = 0 \tag{28}$$

$$\frac{\partial}{\partial x}\langle|\vec{u_0}|^{(b-1)}u_0\rangle + \frac{\partial}{\partial y}\langle|\vec{u_0}|^{(b-1)}v_0\rangle = 0. \tag{29}$$

Of course it has to be demonstrated that solutions of this system exist, since formally, equations (26)–(29) are four equations for three unknowns.

It is not possible to find a closed solution of this problem. However since δ is small, we may expand the coefficients ψ_n in expansion (24) in powers of δ

$$\psi_n = \psi_{n0} + \delta\psi_{n1} + \delta^2\psi_{n2} + \ldots \quad \text{for } n = 0, 1, 2, \ldots . \tag{30}$$

Application to equations (26)–(29), which define the basic state, yields in 0th order

$$\frac{\partial\zeta_{00}}{\partial x} = 0, \qquad \frac{\partial\zeta_{00}}{\partial y} = 0, \qquad \frac{\partial u_{00}}{\partial x} + \frac{\partial v_{00}}{\partial y} = 0 \tag{31}$$

and

$$\frac{\partial}{\partial x}\langle|\vec{u_{00}}|^{(b-1)}u_{00}\rangle + \frac{\partial}{\partial y}\langle|\vec{u_{00}}|^{(b-1)}v_{00}\rangle = 0. \tag{32}$$

A possible solution is

$$u_{00} = \hat{u}_0(t), \qquad v_{00} = \hat{v}_0(t), \qquad \zeta_{00} = \hat{\zeta}_0(t), \tag{33}$$

where the time dependence is determined by the boundary conditions. This solution

describes a spatially uniform tide over a flat bottom. Higher order corrections in δ describe the effects of the slow spatial variation of the tidal wave.

3.2. *Derivation of the linear stability problem*

Since we have expressed the basic state as a series in the small parameter δ, it is consistent to expand the perturbation in powers of δ as well, so in order to determine the solution up to some given accuracy we have to relate the parameters γ and δ. However, for the moment we are mainly interested in the instability mechanism and not in the finite amplitude behaviour of the perturbations. Therefore we limit ourselves to a linear analysis. The problem for ψ_1 reads

$$\frac{\partial \zeta_1}{\partial x} + \delta\left\{\frac{\partial u_1}{\partial t} + u_0\frac{\partial u_1}{\partial x} + u_1\frac{\partial u_0}{\partial x} + v_0\frac{\partial u_1}{\partial y} + v_1\frac{\partial u_0}{\partial y} - \hat{f}v_1 + \hat{r}\left[\frac{u_1}{1+\delta\zeta_0} + \frac{u_0h_1 - \delta u_0\zeta_1}{(1+\delta\zeta_0)^2}\right]\right\} = 0 \tag{34}$$

$$\frac{\partial \zeta_1}{\partial y} + \delta\left\{\frac{\partial v_1}{\partial t} + u_0\frac{\partial v_1}{\partial x} + u_1\frac{\partial v_0}{\partial x} + v_0\frac{\partial v_1}{\partial y} + v_1\frac{\partial v_1}{\partial y} + \hat{f}u_1 + \hat{r}\left[\frac{v_1}{1+\delta\zeta_0} + \frac{v_0h_1 - \delta v_0\zeta_1}{(1+\delta\zeta_0)^2}\right]\right\} = 0 \tag{35}$$

$$\delta\frac{\partial \zeta_1}{\partial t} + \frac{\partial}{\partial x}\left\{(1+\delta\zeta_0)u_1 + \delta\zeta_1u_0 - h_1u_0\right\} + \frac{\partial}{\partial y}\left\{(1+\delta\zeta_0)v_1 + \delta\zeta_1v_0 - h_1v_0\right\} = 0 \tag{36}$$

$$\frac{\partial h_1}{\partial \tau} + \frac{\partial}{\partial x}\left[|\vec{u_0}|^{b-1}u_1 + (b-1)|\vec{u_0}|^{b-3}u_0(u_0u_1 + v_0v_1) - |\vec{u_0}|^b\hat{\lambda}\frac{\partial h_1}{\partial x}\right]$$
$$+ \frac{\partial}{\partial y}\left[|\vec{u_0}|^{b-1}v_1 + (b-1)|\vec{u_0}|^{b-3}v_0(u_0u_1 + v_0v_1) - |\vec{u_0}|^b\hat{\lambda}\frac{\partial h_1}{\partial y}\right] = 0. \tag{37}$$

Approximate solutions of this linear stability problem are obtained from using expansion (30). The $O(\gamma^1\delta^0)$ problem becomes

$$\frac{\partial \zeta_{10}}{\partial x} = 0. \qquad \frac{\partial \zeta_{10}}{\partial y} = 0, \qquad \frac{\partial u_{10}}{\partial x} + \frac{\partial v_{10}}{\partial y} - \hat{u}_0\frac{\partial h_{10}}{\partial x} - \hat{v}_0\frac{\partial h_{10}}{\partial y} = 0 \tag{38}$$

and

$$\frac{\partial h_{10}}{\partial \tau} + \frac{\partial}{\partial x}\left\langle|\vec{\hat{u}_0}|^{b-1}u_{10} + (b-1)|\vec{\hat{u}_0}|^{b-3}\hat{u}_0(\hat{u}_0u_{10} + \hat{v}_0v_{10}) - |\vec{\hat{u}_0}|^b\hat{\lambda}\frac{\partial h_{10}}{\partial x}\right\rangle$$
$$+ \frac{\partial}{\partial y}\left\langle|\vec{\hat{u}_0}|^{b-1}v_{10} + (b-1)|\vec{\hat{u}_0}|^{b-3}\hat{v}_0(\hat{u}_0u_{10} + \hat{v}_0v_{10}) - |\vec{\hat{u}_0}|^b\hat{\lambda}\frac{\partial h_{10}}{\partial y}\right\rangle = 0. \tag{39}$$

Because of the tidal boundary conditions we have $\zeta_{10} = 0$. It is obvious that equations (38) and (39) are not a closed set of equations for u_{10}, v_{10} and h_{10}. Therefore we consider the $O(\delta\gamma)$ momentum equations as well, which read

$$\frac{\partial \zeta_{11}}{\partial x} - \frac{\partial u_{10}}{\partial t} + \hat{u}_0\frac{\partial u_{10}}{\partial x} + \hat{v}_0\frac{\partial u_{10}}{\partial y} - \hat{f}v_{10} + \hat{r}(u_{10} + \hat{u}_0h_{10}) = 0, \tag{40}$$

$$\frac{\partial \zeta_{11}}{\partial y} - \frac{\partial v_{10}}{\partial t} + \hat{u}_0 \frac{\partial v_{10}}{\partial x} + \hat{v}_0 \frac{\partial v_{10}}{\partial y} + \hat{f} u_{10} + \hat{r}(v_{10} + \hat{v}_0 h_{10}) = 0. \tag{41}$$

Here we have used that $\hat{u}_0$ and $\hat{v}_0$ are only functions of time. The new variable ζ_{11} can be eliminated, yielding the vorticity equation

$$\frac{\partial \eta_{10}}{\partial t} + \hat{u}_0 \frac{\partial \eta_{10}}{\partial x} + \hat{v}_0 \frac{\partial \eta_{10}}{\partial y} = -\hat{r}\left[\eta_{10} + \hat{v}_0 \frac{\partial h_{10}}{\partial x} - \hat{u}_0 \frac{\partial h_{10}}{\partial y}\right] - \hat{f}\left\{\frac{\partial u_{10}}{\partial x} + \frac{\partial u_{10}}{\partial y}\right\}, \tag{42}$$

$$\eta_{10} = \frac{\partial v_{10}}{\partial x} - \frac{\partial u_{10}}{\partial y}. \tag{43}$$

Equations (38), (39), (43) and (42) are a closed set of equations for η_{10}, u_{10}, v_{10} and h_{10}. Note that they are coupled since the vorticity field responds to the bottom topography whereas the morphological evolutions are controlled by the flow field. On the tidal time scale, the bottom topography may be treated as being time independent. Thus, for a given initial disturbance the flow response is computed and substitution in the bottom evolution equation then yields the initial growth rate of the bottom. In principle higher order systems in γ yield non-linear corrections. They are not considered this moment but will be analysed in a forthcoming paper. The analysis presented so far is a formal treatment of the intuitive idea that the length scale of the bottom variations is much smaller than the tidal wave length, as has been used by ZIMMERMAN (1980), HUTHNANCE (1982a,b) in their treatment of the tidal ridges, and also by BLONDEAUX (1990), and VITTORI and BLONDEAUX (1990, 1992) in their study on the formation of ripples due to sea waves.

4. SOLVING THE LINEAR PROBLEM

4.1. Working out the linear problem

The linear problem is described by equations (38), (39), (43) and (42). We Fourier transform the unknowns as follows

$$\begin{aligned} u_{10} &= \int\int \tilde{u}(\vec{k},t) e^{-i\vec{k}\cdot\vec{x}} d\vec{k} + cc \qquad & v_{10} &= \int\int \tilde{v}(\vec{k},t) e^{-i\vec{k}\cdot\vec{x}} d\vec{k} + cc \\ \eta_{10} &= \int\int \tilde{\eta}(\vec{k},t) e^{-i\vec{k}\cdot\vec{x}} d\vec{k} + cc \qquad & h_{10} &= \int\int \tilde{h}(\vec{k},t) e^{-i\vec{k}\cdot\vec{x}} d\vec{k} + cc. \end{aligned} \tag{44}$$

The two-dimensional wave vector $\vec{k}$ expressed in Cartesian coordinates is

$$\vec{k} = \begin{pmatrix} k \\ l \end{pmatrix}. \tag{45}$$

Within the constraints of equation (33), we are free to choose a certain basic state. We will investigate the stability of a basic state described by a M_2 tidal ellipse

$$\hat{u}_0(t) = \sin t, \qquad \hat{v}_0(t) = \varepsilon \cos t, \tag{46}$$

in which $\varepsilon = 0$ corresponds to a uni-directional tide and $|\varepsilon| = 1$ to a circular tide. So the x-axis is chosen to coincide with the principal direction of the tidal current. Substituting Eqns (45) and (46) in the continuity equation and the definition of the vorticity we find

$$\tilde{v} = (k^2 + l^2)^{-1}\left(ik\tilde{\eta} + l(k \sin t + l\varepsilon \cos t)\tilde{h}\right) \tag{47}$$

$$\tilde{u} = (k^2 + l^2)^{-1}\left(-il\tilde{\eta} + k(k \sin t + l\,\varepsilon \cos t)\tilde{h}\right). \tag{48}$$

Substitution of equations (45), (47) and (48) in the vorticity equation (42) and the bottom evolution equation (39) yields

$$\frac{\partial \tilde{\eta}}{\partial t} - (ik \sin t + il\varepsilon \cos t - \hat{r})\tilde{\eta} = i\tilde{h}\left[(k\hat{r} + l\hat{f})\,\varepsilon \cos t + (-l\hat{r} + k\hat{f}) \sin t\right] \tag{49}$$

$$\frac{\partial \tilde{h}}{\partial \tau} = -\left\{\hat{\lambda}(k^2 + l^2)\,(\sin^2 t + (\varepsilon \cos t)^2)^{b/2}\tilde{h} + \frac{(b-1)}{(k^2 + l^2)}\left[\tfrac{1}{2}(k^2 - l^2)\,\varepsilon \sin 2t + lk((\varepsilon \cos t)^2 - \sin^2 t)\right](\sin^2 t + (\varepsilon \cos t)^2)^{(b-3)/2}\tilde{\eta}\right\}. \tag{50}$$

Now the problem is more or less decoupled, since bottom topography is assumed not to vary on a tidal-time scale. Thus we can first solve the vorticity equation (49), and substitute this solution into the bottom evolution equation (50). In the remaining part of this section we will examine different ways to solve the vorticity equation, the results of the linear problem will be presented in the next section.

In equation (49) we see that the interaction of the basic flow with the bottom topography causes the generation of vorticity which is oscillatory in the basic tidal frequency, as has already been shown by ZIMMERMAN (1981) and ROBINSON (1981). This forcing is due to the occurrence of torques induced by the Coriolis force and the bottom friction force. The advection of tidal vorticity by the basic tidal current, as described by the second term in equation (49), causes the generation of vorticity in all overtones of the basic tidal frequency, including the residual component. This implies that we can write the solution of equation (49) as a Fourier series:

$$\tilde{\eta} = \tilde{h} \sum_{p=-\infty}^{\infty} c_p e^{ipt}, \tag{51}$$

where the coefficients c_p depend on the parameters k, l, ε, $\hat{r}$, and $\hat{f}$. This enables us to write the bottom evolution equation (50) symbolically as:

$$\frac{\partial \tilde{h}}{\partial \tau} = \omega \tilde{h} \tag{52}$$

in which ω is the initial growth rate of the bed form perturbations. We see that once we know the vorticity the growth rate can be obtained by calculating the tidal average of (products of) harmonical components:

$$\omega = -\left\{\hat{\lambda}(k^2 + l^2)\,\langle(\sin^2 t + \varepsilon^2 \cos^2 t)^{b/2}\rangle + \frac{b-1}{(k^2 + l^2)}\left\langle\left[\tfrac{1}{2}(k^2 - l^2)\,\varepsilon \sin 2t + lk\,(\varepsilon^2 \cos^2 t - \sin^2 t)\right](\sin^2 t + \varepsilon^2 \cos^2 t)^{b-3)/2} \sum_{p=-\infty}^{\infty} c_p e^{ipt}\right\rangle\right\}. \tag{53}$$

4.2. *Exact and truncated solutions of the vorticity equation*

For the extreme cases of the basic flow velocity, $\varepsilon = 0, 1,$ or -1, it is possible to solve the

vorticity equation exactly. ZIMMERMAN (1980) has shown this for anti-clockwise circular tide ($\varepsilon = -1$). In Appendix A we solve the vorticity equation for a uni-directional tide ($\varepsilon = 0$) in a similar way. The result is a solution of the type (51) where

$$c_p = -\frac{(k\hat{f} - l\hat{r})}{\sqrt{k^2 + l^2}} \frac{i^{(p-1)}}{2} \sum_{m=-\infty}^{\infty} J_m(k) \left\{ \frac{J_{m+p+1}(k)}{i(1+m) + \hat{r}} + \frac{J_{m+p-1}(k)}{i(1-m) + \hat{r}} \right\}, \tag{54}$$

and $J_m(k)$ are Bessel-functions of the first kind, order m.

An exact solution of the vorticity equation is only possible for special basic states, and even then it is rather complicated. Therefore we will examine another, approximate method for solving the equation (49). This method will be demonstrated for a general elliptical tide. In the next subsection we will consider the special case of a uni-directional tide in order to compare the solution with the exact solution which we showed in equations (51) and (53).

The technique we will use here to get an approximate solution is harmonic truncation, see LODER (1980) and DE SWART and ZIMMERMAN (1993). The idea is to take only the dominating terms of the series in the Fourier representation

$$\tilde{\eta}_{trunc} = \tilde{h} d_0 + \tilde{h} \sum_{p=1}^{N} (d_{sp} \sin pt + d_{cp} \cos pt). \tag{55}$$

DE SWART and ZIMMERMAN (1993) showed that the cut off must take place after an odd mode, so N must be odd. In many cases an $N = 1$ truncation will yield satisfactory results. However, this excludes the presence of overtides which are known to play an important role in the net transport of sediments (PINGREE and MADDOCK, 1979). Therefore we will also consider an $N = 3$ truncation. We will now explicitly show the procedure for $N = 1$*; in this case we have the formal solution

$$\tilde{\eta}_{trunc} = \tilde{h}[d_0 + d_{s1} \sin t + d_{c1} \cos t] \tag{56}$$

in which the constants d_0, d_{s1} and d_{c1} must be computed. Substituting this formal solution into the vorticity equation, we obtain a set of three algebraic equations for the three unknowns

$$\begin{pmatrix} \hat{r} & -\frac{ik}{2} & -\frac{i\varepsilon l}{2} \\ -ik & \hat{r} & -1 \\ -il & 1 & \hat{r} \end{pmatrix} \begin{pmatrix} d_0 \\ d_{s1} \\ d_{c1} \end{pmatrix} = \begin{pmatrix} 0 \\ i(-\hat{r}l + \hat{f}k) \\ i\varepsilon(\hat{r}k + \hat{f}l) \end{pmatrix}. \tag{57}$$

The solution reads

$$d_0 = (2 + k^2 + \varepsilon^2 l^2 + 2\hat{r}^2)^{-1} (-\hat{f}k^2 + kl\hat{r} - \varepsilon k^2 - \varepsilon l^2 - \varepsilon^2 \hat{f} l^2 - \varepsilon^2 kl\hat{r}) \tag{58}$$

$$d_{s1} = (2 + k^2 + \varepsilon^2 l^2 + 2\hat{r}^2)^{-1} i(2\hat{f}k\hat{r} - 2l\hat{r} + 2\varepsilon\hat{f}l - \varepsilon^2 k^2 l - \varepsilon l^3 + 2\varepsilon k\hat{r}) \tag{59}$$

$$d_{c1} = (2 + k^2 + \varepsilon^2 l^2 + 2\hat{r}^2)^{-1} i(-2\hat{f}k + 2l\hat{r} + \varepsilon k^3 + \varepsilon k l^2 + 2\varepsilon\hat{f}l\hat{r} + 2\varepsilon k\hat{r}) \tag{60}$$

*The expressions for the constants in case of $N = 3$ can be obtained from the first author.

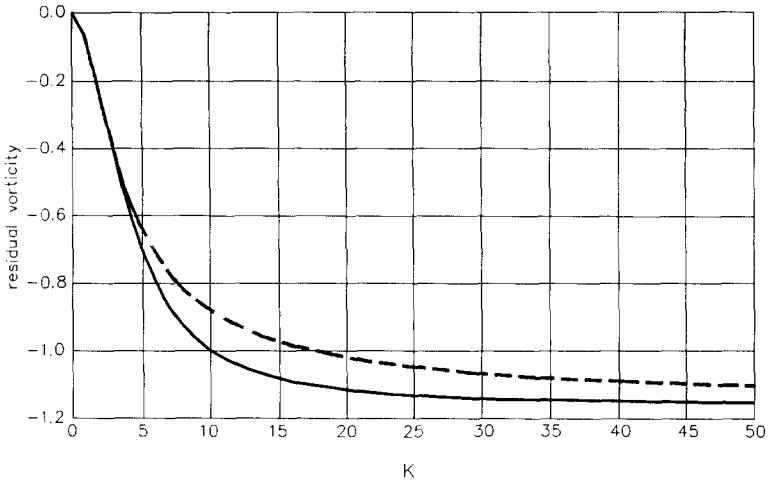

Fig. 3. Residual vorticity response, generated by the interaction of a uni-directional tidal current with the bottom topography, as a function of the wavenumber K of the bed forms for the parameter values $\hat{f} = 0.8$ and $\hat{r} = 0.9$. Here the angle between wavevector and the tidal current is $\theta = 0$. The dashed curve represents the exact solution of c_0 given in equation (55), whereas the solid curve is the approximate solution d_0 presented in equation (58).

4.3. *Comparing the exact and truncated vorticity*

A comparison between the two solutions can only be made in case of a circular or a uni-directional basic tide. Here explicit results are shown for the residual vorticity response in case of a unidirectional tide. In Appendix A it is shown that both the truncated residual vorticity and the exact residual vorticity have the same asymptomatic behaviour for large and small values of the wavenumbers k and l.

As a specific example we have chosen the parameter values $\hat{f} = 0.8$ and $\hat{r} = 0.9$ which correspond to a physically realistic situation, as was discussed at the end of section 2.

We change to polar coordinates for the wavevector:

$$\vec{k} = \begin{pmatrix} k \\ l \end{pmatrix} = \begin{pmatrix} K\cos\theta \\ K\sin\theta \end{pmatrix}. \tag{61}$$

In Fig. 3 a plot of the exact and approximate residual vorticity response is shown for $\theta = 0$.

The plot for the other angles is similar. For moderate values of the length of the wave vector K the exact solution makes some oscillations, which do not occur in the truncated solution. However, the general agreement between the two solutions is satisfactory. This conclusion also holds as far as the response in the basic tidal frequency is concerned.

Obviously the truncated solution of the residual vorticity behaves, except for some small oscillations, the same as the exact solution for a uni-directional tide. Since the truncation technique also works well in other applications (see DE SWART and ZIMMERMAN, 1993) we will use it to solve the vorticity equation in this paper, without explicitly proving the equality with the exact solution.

5. RESULTS

Now that we have solved the flow response we are able to determine the behaviour of the bed disturbances. The uni-directional tide ($\varepsilon = 0$) yields exponentially growing and

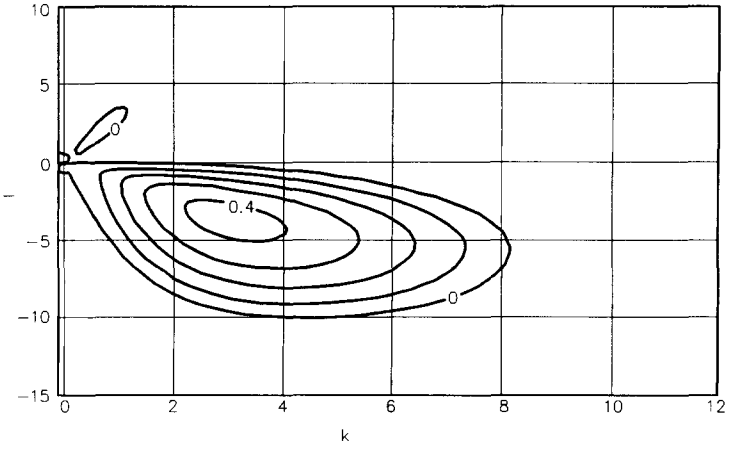

Fig. 4. Contour plot of the growth rates of bed form perturbations, calculated from equation (63), in the (k,l) wavenumber plane for a uni-directional tide ($\varepsilon = 0$). The other parameters are $b = 3, \hat{f} = 0.82, \hat{r} = 0.6$ and $\hat{\lambda} = 0.01$.

decaying disturbances depending on the wavevector $\vec{k}$ of the disturbance. If we make the choice $b = 3$, and substitute the vorticity response, obtained from an $N = 3$ truncation, we can compute the initial growth rate from equation (53)

$$\omega = -\left\{\frac{kl}{2(k^2 + l^2)}[2d_0 - d_{c2}] + \frac{4\hat{\lambda}}{3\pi}(k^2 + l^2)\right\}, \tag{62}$$

where the coefficients d_n are defined in equation (55). The first term on the right hand side describes the net convergence of the sediment flux due to the topographically induced circulations. The latter consists of a residual part and an M_4 component (first overtide), as indicated by the coefficients d_0 and d_{c2}, respectively. In Fig. 4 contour lines of the growth rate are shown in the wavenumber space for the model parameters $\hat{f} \simeq 0.8, \hat{r} \simeq 0.6$ and $\hat{\lambda} \simeq 0.01$. They roughly represent North Sea conditions (see the discussion at the end of section 2). A dimensionless growth rate corresponds to an e-folding time scale of T_m/ω, where the morphological time scale is defined in equation (20).

The initially fastest growing mode is $K \sim 5$, which in this case corresponds to a dimensional wave-length of approximately 8 km, and the direction $\theta \sim 60°$ where θ is defined in equation (61). We remark that the very long waves are also exponentially growing, although with smaller growth rates. Experiments demonstrated that the growth rates are mainly determined by the residual circulations around the banks. The response of the first overtide is only of marginal importance.

There model results are in agreement with those of HUTHNANCE (1982a,b) and DE VRIEND (1990) and compare reasonably well with the observed scales and orientation of tidal ridges in shallow seas. The main difference between the various models is the applied parameterization of the sediment transport and the way in which the tidal flow equations are solved.

The physical mechanism of bank formation may be explained as follows, see also HUTHNANCE (1982a,b). A tidal current moving over a bank crest experiences an anticyclonic residual circulation. As the orientation of the bank is slightly cyclonic with respect to the flow direction the total flow velocity is slightly increased upstream of the crest whereas

it is decreased downstream of the crest. Since the sediment flux is proportional to some power of the flow velocity there is a net convergence of sediment at the crest causing a growth of the bank. This growth is only counteracted by the bed slope correction term in the sediment transport equation which becomes effective for short waves.

Note that the models only predict the growth of large-scale tidal ridges, i.e. no sand waves are found. Furthermore, it appears that if a model parameter, such as the friction coefficient $\hat{r}$, is varied it follows that the first modes which become unstable correspond to ultra-long waves. This is contrary to observations which demonstrate that for sufficiently small tidal current amplitudes or large water depths no bed forms are found, and the largest known wave-length of tidal sand banks is about 20 km (OFF, 1963). In order to include these effects we have modified our model by allowing for elliptical tidal current. In case of a cyclonic circular tide ($\varepsilon = -1$) we obtain for the initial growth rate of bed perturbations (expressed in polar coordinates)

$$\omega = \tfrac{1}{2} d_{s2}(k = K, l = 0) - \lambda K^2. \tag{63}$$

A plot for the same other parameter values as where considered for the uni-directional tide, is shown in Fig. 5.

It is remarkable that the growth of sand banks is now determined by the first overtide only. Although there will be residual circulations around the banks they do not contribute to the net transport of sediment. The reason for this behaviour is that the banks do not have any preferred direction with respect to the tidal current. Thus, if at a specific time, due to the residual circulations, there is a net convergence of sediment at the crests there is another time during the tidal cycle at which there is the same amount of sediment flux divergence at the crest.

The mechanism of the bed form growth in the case of circular tides can be understood as follows. Basically the topography causes the generation of tidal vorticity due to the Coriolis torque and the bottom frictional torque. Since these forcing terms are determined by the flow components perpendicular and parallel to the depth contours, respectively, they now have a phase difference of 90°. Together with the inertial effects this causes the tidal vorticity to have a phase difference with the tidal velocity component over the depth contours. Advection of this vorticity by the basic tidal current will cause the generation of both a residual vorticity field and a response in the first overtide. It has already been argued that for the net transport of sediments only the first overtide is important. Therefore, the effect of the first overtide circulation on the total flow velocity and the resulting divergences in the sediment fluxes must be computed. In fact this procedure is similar to the previous case of a uni-directional tide where the effect of the residual circulation was investigated. As a result it is found that bank growth can only occur if the tidal current has a cyclonic polarization ($\varepsilon = -1$). In case of an anticyclonic polarization the phase difference between the tidal current and the circulation in the first overtide is such that there is merely divergence of sediment fluxes at the crests of the banks.

As the circular tide has no preferred direction, we can determine only the growth rate as a function of K. Figure 5 shows that the fastest growing mode is $K \sim 5$ which in this case corresponds with a dimensional wave-length of 8 km.

Figure 6 shows the marginal stability curve for cyclonic circular tide. This curve is defined as the contour $\omega = 0$ and separates exponentially growing and decaying perturbations. It shows there is a certain wavenumber which is the first one that becomes unstable if we increase the friction parameter. The difference between the uni-directional

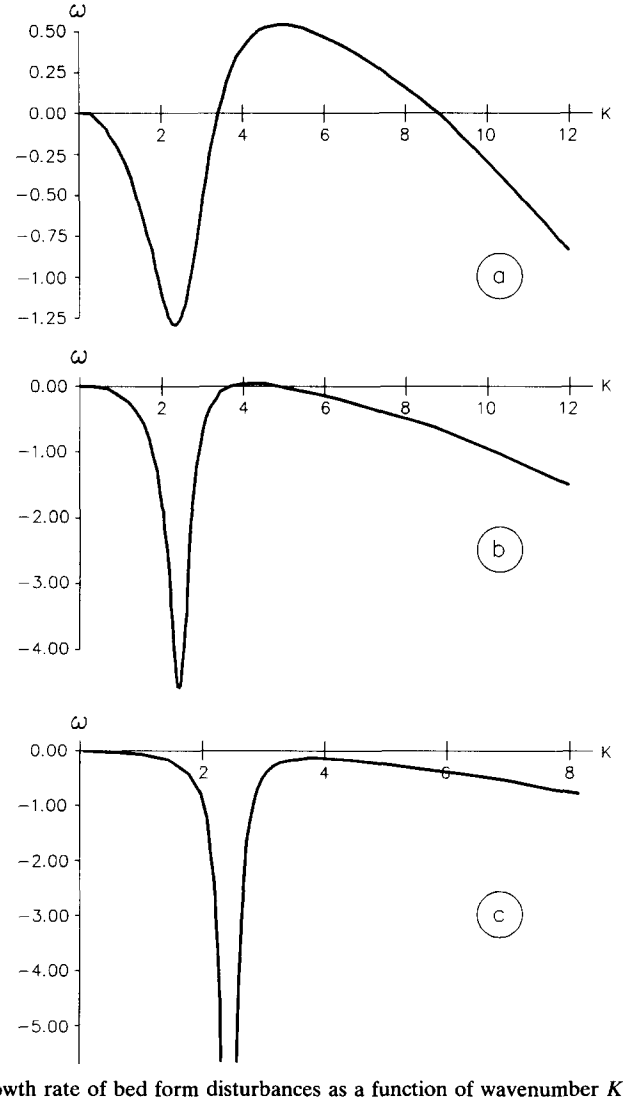

Fig. 5. Growth rate of bed form disturbances as a function of wavenumber K for a cyclonical circular tide ($\varepsilon = -1$) for the friction parameters $\hat{r} = 0.5$ (a), $\hat{r} = 0.2$ (b) and $\hat{r} = 0.1$ (c). Other parameter values as in Fig. 4.

and circular tide is the growth rate of the long waves. Long waves are always suppressed in case of a circular tide, where as they are the first to grow in case of a uni-directional tide. This is caused by the fact that the net sediment transports in case of a uni-directional tidal current are determined by the residual currents. Since the latter behave as K^2 for $K \to 0$, the growth of bed forms cannot be compensated for by the stabilizing bed slope correction term in the transport formula. On the other hand the net sediment transport in case of a circular tide is determined by the first overtide, which behaves as K^4 for $K \to 0$. We conclude that a model with elliptical tides will predict only growing bed form perturbations if the model parameters are larger than certain critical values. In that case the crests of the

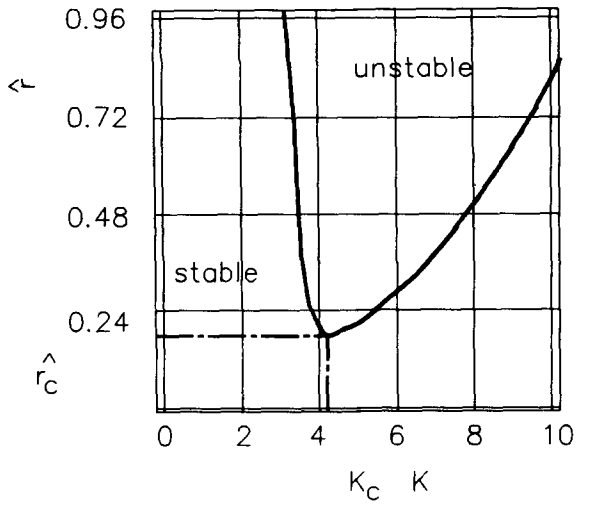

Fig. 6. Neutral stability curve for a cyclonic circular tide. The curve separates exponentially growing and decaying perturbations in the $(K,\hat{r})$ plane, where K is the wavenumber and $\hat{r}$ the bottom friction parameter. Other parameter values as in Fig. 4.

preferred disturbances will be cyclonically orientated with respect to the principal tidal current direction.

6. SAND WAVES

The model's inability to predict the growth of smaller features (sand waves, megaripples, dunes, ripples) sand waves is probably caused by the fact that the vertical structure of the currents is not taken into account (also see RICHARDS, 1980). The depth-averaged flow equations are based on a strict similarity assumption for the velocity distribution over the vertical, for instance a logarithm. This leads to the relationship between the bed shear stress and the depth-averaged current velocity which closes the mathematical system.

The flow field which can be constructed from the depth-averaged velocity and the standard vertical profile will be called the "primary flow". In principle, all accelerations of this primary flow induce secondary circulations in the vertical which make the velocity distribution deviate from that in plane uniform shear flow. Hence they also affect the bed shear stress and the sediment transport.

If only the effects of the curvature and the downstream advective acceleration of the primary flow are taken into account, the bed shear stress in the case of fully-developed secondary flow is given by (see DE VRIEND, 1977):

$$\tau_{bs} = \tau_{b0}\left[1 + f_{sec}\frac{H-h+\zeta}{U}\frac{\partial U}{\partial s}\right] \tag{64}$$

$$\tau_{bn} = \tau_{b0} f_{sec}\frac{H-h+\zeta}{R_s}, \tag{65}$$

in which τ_{bs} and τ_{bn} are the (dimensional) shear stress components in the downstream and cross-stream direction, respectively, τ_{b0} is the (quadratic) shear stress due to the main

flow, U is the total depth-averaged velocity, s is the metric coordinate along the streamlines of the main flow, and R_s is the radius of curvature of those streamlines. The factor f_{sec} is a constant which follows from secondary flow theory (see DE VRIEND, 1977).

When transformed to cartesian coordinates, the above expressions become (see DE VRIEND, 1977)

$$\tau_{bx} = \tau_{b0}\left[\frac{u}{U} + f_{sec}\frac{H-h+\zeta}{U^2}\left(u\frac{\partial u}{\partial x} + v\frac{\partial u}{\partial y}\right)\right] \tag{66}$$

$$\tau_{by} = \tau_{b0}\left[\frac{v}{U} + f_{sec}\frac{H-h+\zeta}{U^2}\left(u\frac{\partial v}{\partial x} + v\frac{\partial v}{\partial y}\right)\right]. \tag{67}$$

Rewriting the sediment transport formula in terms of the bed shear stress yields

$$\vec{S_b} = \alpha'|\vec{\tau_b}|^{b'}\left\{\frac{\vec{\tau_b}}{|\vec{\tau_b}|} - \lambda\vec{\nabla}h\right\}. \tag{68}$$

in which α' and b' are modifications of α and b, respectively, depending on the choice of the bed shear stress formula. As the shear stress due to the secondary flow is small relative to that to the primary flow, it is sufficient to retain only first-order terms when substituting equations (66) and (67) into (68). The result reads

$$\vec{S_b} = \alpha'\tau_{b0}^{b'}\left[\frac{\vec{u}}{|\vec{u}|} - \lambda\vec{\nabla}h + f_{sec}\frac{H-h+\zeta}{U^2}\begin{pmatrix}\left(u\frac{\partial u}{\partial x} + v\frac{\partial u}{\partial y}\right)\\ \left(u\frac{\partial v}{\partial x} + v\frac{\partial v}{\partial y}\right)\end{pmatrix}\right]. \tag{69}$$

For $f_{sec} = 0$, this reduces to the transport formula in equation (5).

Following the linearization procedure described in section 3, a set of differential equations can be derived for the flow perturbations due to a small bed wave of a given wave length and orientation. In order to have a first impression of the secondary flow effects, these equations were solved numerically for a uni-directional tide over long-crested bed waves. The results were used to calculate the growth rate and the celerity of those waves, much along the lines described before [see equations (39) and (52)]. A more detailed description of this procedure, is given by DE VRIEND (1990).

Exploratory computations with this model led to the following observations

—The inclusion of the acceleration effects causes the growth of a new class of bed forms with an essentially shorter wave-length than the tidal ridges [see Fig. 7(a) and (b)].

—The downstream acceleration of the primary flow has the strongest effect on bed forms with their crests perpendicular to the flow. In that case, it causes a residual uphill transport which enhances the bed's instability to short wave-lengths, event to the extent that the shortest waves tend to grow fastest [see Fig. 7(b)].

—The curvature-induced secondary flow has its strongest effect on bed forms with their crests under an oblique angle with the primary flow, but not to the extent that this creates another maximum in the growth rate [see Fig. 7(b)].

The above results are found if the secondary flow is always and everywhere fully developed. If the spatial variations of the primary flow are too fast, however, the secondary flow cannot follow them, because of its own inertia. The extension of the model

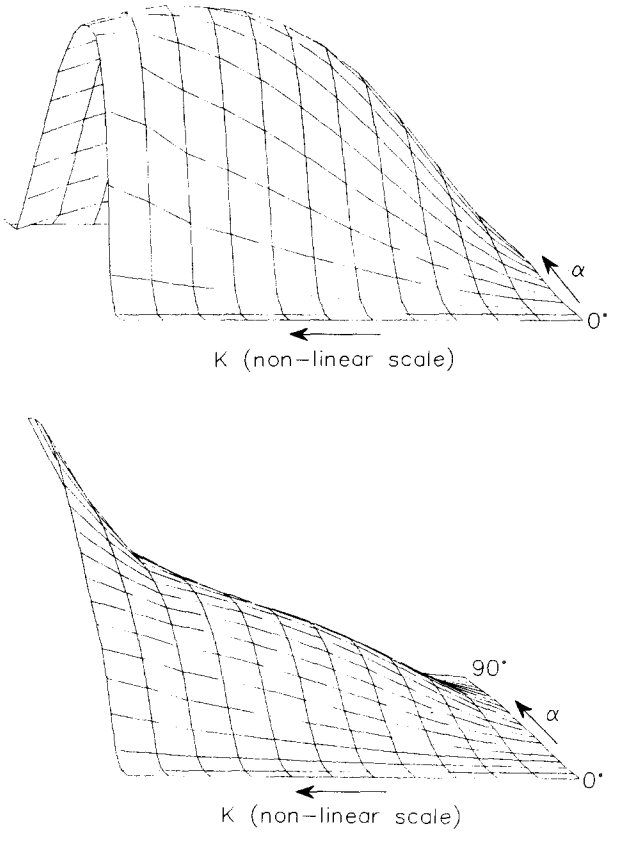

Fig. 7. Growth rate of a uni-directional tide under an angle θ with the crest of a bed wave with wave number K, (a) secondary flow disregarded, (b) fully-developed secondary flow included. Note that the wavenumber axis is distorted (k is unevenly distributed along the axis) and that the vertical scales are different in the two parts of the figure.

to shorter wave-lengths therefore requires the inclusion of this inertia effect. DE VRIEND (1981) has shown that this can be done approximately as follows:

—the bed shear stress is rewritten into the generalized form

$$\tau_{bs} = \tau_{b0}\left[1 + f'_{sec}\frac{I_s}{U}\right] \tag{70}$$

$$\tau_{bn} = \tau_{b0} f'_{sec}\frac{I_n}{U}, \tag{71}$$

in which I_s and I_n denote the intensities of the downstream and cross-stream secondary flow components, respectively, and f'_{sec} is a known constant;

—the secondary flow intensities are described by the relaxation equations

$$\frac{\partial I_s}{\partial s} + \frac{I_s}{\lambda_s} = f''_{sec}\frac{H - h + \zeta}{\lambda_s}\frac{\partial U}{\partial s} \tag{72}$$

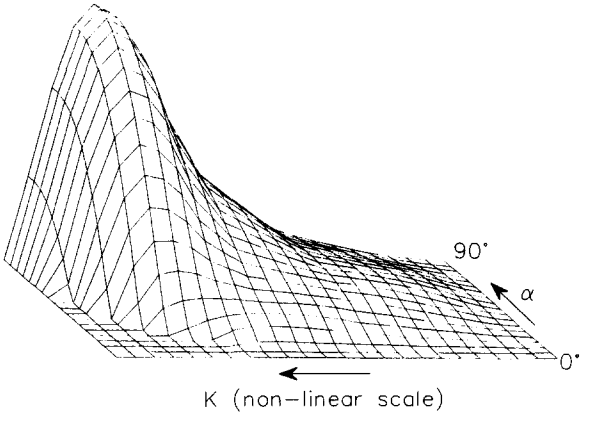

Fig. 8. As Fig. 7, but with the inertia of the secondary flow included. Note that the wavenumber axis is extended with respect to that of Fig. 7, and that the vertical scale is different.

$$\frac{\partial I_n}{\partial s} + \frac{I_n}{\lambda_s} = f''_{sec} \frac{H - h + \zeta}{\lambda_s} \frac{U}{Rs} \tag{73}$$

in which f''_{sec} is another known constant and λ_s is the inertial adjustment length for the secondary flow intensity;

—the adjustment length is approximated by

$$\lambda_s = 0.6(H - h + \zeta) \frac{1}{\sqrt{f_{sh}}} \tag{74}$$

in which f_{sh} denotes the friction factor in the expression for τ_{b0}.

This parametric model has been validated for steady flow in river bends (STRUIKSMA *et al.*, 1985), but to what extent it also applies to tidal flow remains to be investigated. Yet, it gives at least a qualitative indication of the effects of secondary flow inertia.

If the linear stability analysis for the uni-directional tide is repeated with this extended secondary-flow model, there is a maximum in the growth rate of the shorter modes (see Fig. 8), at wave-lengths which are of the same order of magnitude as those of sand waves.

The above preliminary analysis gives an indication of the effects of secondary flows, but it cannot be final. Likewise the analysis of tidal ridges in the foregoing, it has to be redone more accurately, if possible analytically, in order to have a basis for further non-linear analyses.

7. CONCLUSIONS

In this paper we have investigated a mechanism which may cause the formation of sand waves and ridges in shallow seas. We have demonstrated that free instabilities of a simple morphological system have many characteristics similar to observed sand waves and ridges. In case of a uni-directional tide we obtain results which are in agreement with those found by HUTHNANCE (1982a,b) and DE VRIEND (1990).

Two limitations of these models have been discussed, *viz.* the absence of critical model parameters below which the basic tidal current is stable and the inability to predict the

growth of sand waves. Therefore we have introduced modifications of the model by including the effect of secondary currents in the sediment transport and by allowing for elliptical tidal currents. The effect of secondary currents on the direction of the sediment flux causes the growth of both sand waves and sand ridges. The ellipticity of the tide yields a critical parameter setting below which all bed form growth is suppressed. In case of a circular tide the wave-length of the critical mode is approximately 8 km for a parameter setting which is typical for the North Sea.

A basic limitation of the presented linear stability analysis is that it is only valid as long as amplitudes of the perturbations are infinitesimally small. Consequently, only information on the initial growth of bed forms is obtained and for investigating the long-term behaviour, when amplitudes have reached finite values, a non-linear analysis is required. In the case of uni-directional tides, for realistic combination of the model parameters a wide spectrum of growing bed forms is found from the linear analysis. A non-linear analysis would then involve interactions between all of these modes and as a result a complex bottom topography with many length scales is to be expected. This is contrary to observations which show rhythmic patterns having one clearly defined wave-length.

In case of a circular tide the presence of critical model parameters enables us to set up a weakly non-linear analysis which will yield a modulation equation. This will describe the envelope amplitude of a group of marginally growing bed form disturbances centered around the critical mode. A similar analysis has been carried out by SCHIELEN *et al.* (1993) for the formation of alternate bars in rivers. The analysis will also yield information on the shape of the bed forms as well as on the possible interaction between sand waves and tidal sand ridges.

Acknowledgements—The work presented herein was carried out as part of the "G8 Coastal Morphodynamics" research programme. It was funded jointly by Delft Hydraulics, in the framework of the Netherlands Centre for Coastal Research, and the Commission of the European Communities, Directorate General for Science, Research and Development, under contract no. MAS2-CT92-0027.

REFERENCES

BLONDEAUX P. (1990) Sand ripples under sea waves, part 1. Ripple formation. *Journal of Fluid Mechanics*, **218**, 1–17.

DE SWART H. E. and J. T. F. ZIMMERMAN (1993) Rectification of the winddriven ocean circulation on the beta plane. *Geophysics and Astrophysics of Fluid Dynamics*.

DE VRIEND H. J. (1977) A mathematical model of steady flow in curved shallow channels. *Journal of Hydraulic Research*, **15**, 37–54.

DE VRIEND H. J. (1981) *Steady flow in shallow channel bends*. Delft University of Technology, Department of Civil Engineering, Communications on Hydraulics 81-3, 260 pp.

DE VRIEND H. J. (1990) Morphological Processes in Shallow Tidal Seas. In: *Residual currents and long term transport*, R. T. CHENG, editor, Verlag, Coastal and Estuarine Studies, **38**, pp. 276–301.

GRADSHTEYN I. S. and I. M. RYZHIK (1980) *Table of integrals, series and products*. Academic Press, 1160 pp.

HUTHNANCE J. (1982a) On one mechanism forming linear sand banks. *Estuarine and Coastal Shelf Science*, **14**, 79–99.

HUTHNANCE J. (1982b) On the formation of sand banks of finite extent. *Estuarine and Coastal Shelf Science*, **15**, 277–299.

KROL M. (1991) On a Galerkin-averaging method for weakly nonlinear wave equations. *Mathematics and Applied Sciences*, **11**, 649–664.

LANCKNEUS J. and G. DE MOOR (1991) Present-day evolution of sand waves on a sandy shelf bank. *Oceanologica Acta*, **11**, 123–127.

LODER J. W. (1980) Topographic rectification of tidal current on the sides of Georges Bank. *Journal of Physical Oceanography*, **10**, 1399–1416.

OFF T. (1963) Rhythmic linear sand bodies caused by tidal currents. *Bulletin of the American Association of Petroleum Geologists*, **47**, 324–341.

PATTIARATCHI C. and M. COLLINS (1987) Mechanisms for linear sandbank formations and maintenance in relation to dynamical oceanographical observations. *Progress in Oceanography*, **19**, 117–156.

PINGREE R. D. and L MADDOCK (1979) The tidal physics of headland flows and offshore tidal bank formation. *Marine Geology*, **32**, 269–289.

RICHARDS K. J. (1980) The formation of ripples and dunes on an erodible bed. *Journal of Fluid Mechanics*, **99**(3), 597–618.

ROBINSON I. S. (1981) Tidal vorticity and residual circulation. *Deep-Sea Research*, **28**, 195–212.

SANDERS J. A. and F. VERHULST (1985) *Averaging methods in non-linear dynamical systems*. Springer-Verlag, 247 pp.

SCHIELEN R., A. DOELMAN and H. E. DE SWART (1993) On the non-linear dynamics of free bars in straight channels. *Journal of Fluid Mechanics*, **252**, 325–356.

STRIDE A. H. (editor) (1982) *Offshore tidal sands: processes and deposits*. Chapman and Hall, London.

STRUIKSMA N., K. W. OLESEN, C. FLOKSTRA and H. J. DE VRIEND (1985) Bed deformation in curved alluvial channels. *Journal of Hydraulic Research*, **23**, 57–79.

VAN ALPHEN J. S. L. J. and M. A. DAMOISEAUX (1989) A geomorphological map of the Dutch shoreface and adjacent part of the continental shelf. *Geologie en Mijnbouw*, **68**, 433–444.

VAN RIJN L. C. (1989) *Handbook of sediment transport by currents and waves*, Delft Hydraulics, Delft, The Netherlands.

VITTORI G. and P. BLONDEAUX (1990) Sand ripples under sea waves, part 2. Finite amplitude development. *Journal of Fluid Mechanics*, **218**, 19–39.

VITTORI G. and P. BLONDEAUX (1992) Sand ripples under sea waves, part 3. Brick pattern ripple formation. *Journal of Fluid Mechanics*, **239**, 23–45.

ZIMMERMAN J. T. F. (1980) Vorticity transfer by tidal currents over an irregular topography. *Journal of Marine Research*, **38**, 601–630.

ZIMMERMAN J. T. F. (1981) Dynamics, diffusion and geomorphological significance of tidal residual eddies. *Nature*, **290**, 549–555.

ZIMMERMAN J. T. F. (1982) On the Lorentz linearization of a quadratically damped forced oscillator. *Physics Letters*, **89A**, 123–124.

APPENDIX A: EXACT SOLUTION OF THE VORTICITY EQUATION

In this appendix we work out explicitly the calculations we need in section 4 to compare the vorticity calculated exactly and approximated by harmonic truncation. We will do this for an uni-directional tide.

(A1). *Exact solution of vorticity equation for a uni-directional tide*

In this case the vorticity equation is

$$\frac{\partial \tilde{\eta}}{\partial t} - (ik \sin t - \hat{r})\tilde{\eta} = \tilde{h}(-il\hat{r} + ik\hat{f}) \sin t. \tag{75}$$

We can solve this inhomogeneous equation with variation of constants. We start with the homogeneous equation:

$$\frac{\partial \tilde{\eta}}{\partial t} - (ik \sin t - \hat{r})\tilde{\eta} = 0, \tag{76}$$

which has the solution

$$\tilde{\eta} = Ce^{-ik \cos t - \hat{r}t}. \tag{77}$$

Now we make the integration constant C dependent on time which enables us to derive an expression for the solution of the inhomogeneous equation:

$$\tilde{\eta} = i\tilde{h}(k\hat{f} - l\hat{r})e^{-ik\cos t - \hat{r}t}\int_{-\infty}^{t} \sin t'\, e^{ik\cos t' + \hat{r}t'}\, dt'. \tag{78}$$

In working out the integration we use the following equality

$$e^{ik\cos t} = \sum_{m=-\infty}^{\infty} i^m e^{imt} J_m(k), \tag{79}$$

in which $J_m(k)$ is the m^{th} order Bessel function of the first kind. Now we are able to give the exact solution:

$$\tilde{\eta} = \tilde{h}\frac{(k\hat{f} - l\hat{r})}{2i} e^{ik\cos t} \sum_{m=-\infty}^{\infty} i^m J_m(k) e^{imt}\left\{\frac{e^{it}}{i(1+m) + \hat{r}} - \frac{e^{it}}{i(1-m) + \hat{r}}\right\}. \tag{80}$$

It will turn out that it is practical to decompose the vorticity in Fourier components:

$$\tilde{\eta} = \tilde{h}\sum_{p=-\infty}^{\infty} c_p e^{ipt}. \tag{81}$$

The results for the coefficients c_p are given in equation (54). The equalities for Bessel functions which are needed are summarized in the Appendix of ZIMMERMAN (1980).

(*A*2). *Calculations to compare vorticities*

With help of the earlier mentioned rules for Bessel functions we can write the expression for the exact solution:

$$c_0 = 2\frac{(-k^2\hat{f} + lk\hat{r})}{(k^2 + l^2)} \sum_{n=1}^{\infty} \frac{n^2 J_n^2(k)}{n^2 + \hat{r}^2}. \tag{82}$$

The truncated residual vorticity for a uni-directional tide becomes

$$d_0 = \frac{-k^2\hat{f} + lk\hat{r}}{2 + k^2 + 2\hat{r}^2}. \tag{83}$$

In the limit that $k \to \infty$ we can compute* the sum in expression (82).

$$\lim_{k\to\infty} \sum_{n=1}^{\infty} \frac{n^2 J_n^2(k)}{n^2 + \hat{r}^2} = \lim_{k\to\infty} \sum_{n=1}^{\infty} J_n^2(k) - \hat{r}^2 \lim_{k\to\infty} \sum_{n=1}^{\infty} \frac{J_n^2(k)}{n^2 + \hat{r}^2} = \lim_{k\to\infty} (\tfrac{1}{2} - \tfrac{1}{2}J_0^2(k)) = \tfrac{1}{2}. \tag{86}$$

Now we are able to compute the expressions for c_0 and d_0 in the formal limit $k \to \infty$ and we obtain that they both become $-f$.

---

*We used that the order of summation can be changed. This is allowed because the sum is absolutely convergent

$$\sum_{n=1}^{\infty} \left|\frac{n^2 J_n^2(k)}{n^2 + \hat{r}^2}\right| = \sum_{n=1}^{\infty} \frac{n^2 J_n^2(k)}{n^2 + \hat{r}^2} \leq \sum_{n=1}^{\infty} \frac{1}{n^2 + \hat{r}^2} \leq \sum_{n=1}^{\infty} \frac{1}{n^2} \leq \int_1^{\infty} \frac{1}{x^2} dx = 1. \tag{84}$$

We also used an equality for Bessel functions (see GRADSHTEYN and RYZHIK, 1980, p. 980):

$$J_0^2(k) + 2\sum_{n=1}^{\infty} J_n^2(k) = 1. \tag{85}$$

$$\lim_{k\to\infty} \sum_{n=1}^{\infty} \frac{n^2 J_n^2(k)}{n^2 + \hat{r}^2} = \lim_{k\to\infty} \sum_{n=1}^{\infty} J_n^2(k) - \hat{r}^2 \lim_{k\to\infty} \sum_{n=1}^{\infty} \frac{J_n^2(k)}{n^2 + \hat{r}^2} = \lim_{k\to\infty} (\tfrac{1}{2} - \tfrac{1}{2}J_0^2(k)) = \tfrac{1}{2}. \tag{86}$$